Journal of Power Sources, *31* (1990) 93 - 106

REFERENCE-ELECTRODE AND GASSING STUDIES OF LEAD/ACID CHARGE-DISCHARGE PROCESSES

J. A. MAGYAR, M. A. KEPROS and R. F. NELSON*
Gates Energy Products, Inc., Sealed Lead Division, Warrensburg, MO (U.S.A.)

Introduction

Reference-electrode measurements combined with gassing and cell current/voltage monitoring can provide considerable information about the mechanism and kinetics of oxygen recombination in valve-regulated lead/acid (VRLA) cells and batteries, a process that is poorly understood at best. Starting with Tafel's initial study on plate polarization as a function of charge conditions [1], the use of reference electrodes to examine individual plate behaviour on charge and discharge has been a powerful research tool. Results from this approach can be augmented by data gleaned from concurrent gas evolution and/or temperature monitoring to gain a deeper understanding of the oxygen cycle in VRLA cells and batteries. This paper presents some preliminary results, obtained on spiral-wound VRLA products, aimed towards discovering how oxygen recombination operates in these systems at the microscopic level.

The oxygen cycle in lead/acid cells begins with the overcharge reaction at the positive electrode where water is decomposed to produce oxygen gas:

$$2H_2O \rightleftharpoons 4H^+ + 4e^- + O_2 \qquad (1)$$

In a flooded battery, this oxygen will escape from the cell along with hydrogen gas being liberated concurrently at the negative electrode, which is also in overcharge. A so-called sealed recombinant lead/acid system is designed so that the positive goes into overcharge before the negative; the negative active material is in excess and oxygen generated at the positive diffuses to the negative and is chemically oxidized in an overall process given by:

$$O_2 + 2Pb + 2H_2SO_4 \rightleftharpoons 2PbSO_4 + 2H_2O \qquad (2)$$

Thus, water is regenerated and the $PbSO_4$ formed is then electrochemically converted back to sponge lead. The major challenge in designing an effective VRLA cell is to facilitate movement of O_2 between the two electrodes via the separator to effect direct plate-to-plate recombination, shown con-

*Author to whom correspondence should be addressed.

0378-7753/90/$3.50

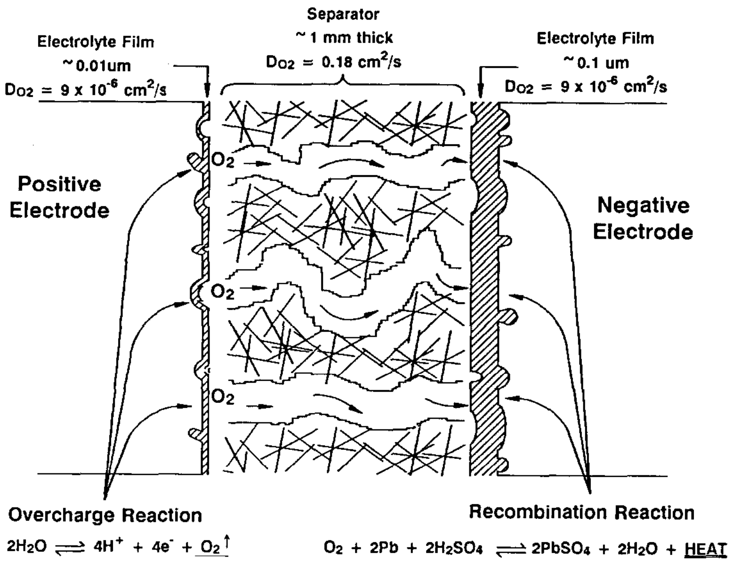

Fig. 1. Conceptual view of oxygen recombination process.

ceptually in Fig. 1. The primary features necessary to accomplish this are:

- excess capacity in the negative plate so that the positive will go into overcharge first
- a thin-film condition in the plate pores to facilitate oxygen egress from the positive and approach to the negative
- substantial void volume in the separator and minimal tortuosity to afford the shortest gas paths between the plates
- firm plate/separator stack pressure to provide intimate contact between the cell elements
- positive absolute internal cell pressure and a one-way vent to allow excess pressure build-up to be dissipated and, at the same time, prevent ingress of atmospheric oxygen.

Rüetschi [2] has shown that, given the film thicknesses, separator dimensions, oxygen solubilities and partial pressures, and gas- and liquid-phase diffusivities involved, the rate-limiting step in oxygen transport is, clearly, penetration of the negative-plate electrolyte film to allow oxygen reaction with the lead surface.

This study is the first attempt to quantify the factors listed above in terms of their impact on recombination efficiency. This first study is focused on the effect of internal cell pressure by variation in the characteristics of the cell vent valves, as well as a general demonstration of the use of reference electrodes in studying VRLA battery/cell performance.

Experimental

All cells and batteries employed were from standard production lots, except for those with modified vent valves; the latter, though, were put through standard processing after modification of the venting systems.

Vent valves were modified for 'D' cells (2 V/2.5 A h) in two ways. The first was by machining down the fill stems over which the Bunsen valves fit; venting pressure is a function of the tightness of fit between the fill stem and the rubber valve; as the fill stem is machined down, the vent pressure will decrease. This created three groups of cells with the venting characteristics shown in Table 1.

It was felt that the surface roughness induced by machining might allow oxygen ingress for the 'low' groups, so a second group of cells was fabricated by putting small slits in the tops of the Bunsen valves. It was expected that these slits would open to allow venting when internal pressures built up, but would not allow air ingress. These 'slit' valves had the venting characteristics given in Table 2.

Both groups were individually tested before cell assembly, and Bunsen valves and cell inner tops/fill stems, once tested together, were assembled together. It is not known whether vent pressures measured on a standard test fixture with compressed air equate exactly to vent pressures in operation, or whether the tested vent pressures are maintained through processing and testing, but it is probably safe to assign qualitative values of 'low', 'medium' or 'high' (production), and this is how they will be referred to in the text.

TABLE 1

	Venting pressures (psi)		
	'Low'	'Medium'	'High'
Number of samples	50	50	50
Mean vent pressure	6.4	14.0	37.2
Standard deviation	1.5	3.0	3.2
Range	3 - 11	6 - 19	27 - 44

TABLE 2

	Venting pressures (psi)	
	'Low'	'Medium'
Number of samples	51	49
Mean vent pressure	5.7	9.6
Standard deviation	1.3	1.5
Range	3 - 7	8 - 13

The cadmium wire used was 0.64 mm-thick reagent-grade material from Alfa Products. In 'D' and 'X' single cells, it was inserted through a small hole in the poly(propylene) cell liner just above the bottom, where it would make contact with the compressed, wetted separator material. Epoxy glue was then used to seal up the plastic/wire insert area. All voltages shown are to be taken as only relative values, as it is conceded that long-term exposure of the cadmium wire to the electrolyte will no doubt shift its 'reference' potential. Work is in progress on developing a mercury/mercurous sulphate reference for use with Gates spiral-wound cells and batteries. Short-term voltage readings were always stable with these electrodes, except when high currents were passed; the resulting highly erratic readings were ascribed to gas bubble formation on the wire surface.

The electrical equipment used for constant-voltage and constant-current overcharge experiments was standard regulated power supplies (Hewlett-Packard) and $4\frac{1}{2}$ digit multimeters (Keithley). Resulting current and voltage data were recorded either with Yokogawa YEW 30-channel recorders or a Hewlett-Packard 7090A recorder/plotter. Potentiostatic experiments were carried out using a Thompson Electrochem, Ltd. Ministat Research Potentiostat Model 402 R. Gas evolution experiments were conducted using castor oil displacement from inverted burettes with manual readings being taken. All volumes were corrected to STP conditions.

Results and discussion

Typically, in flooded lead/acid cells, reference-electrode monitoring shows fairly smooth polarizations of about 80 and 120 mV per decade current increase for the positive and negative electrodes, respectively [3, 4], as the electrodes are driven into the gas evolution regions. In a recombinant system, the oxygen cycle will hold the potential of the negative electrode near the open-circuit value, and on constant-voltage (CV) float charge virtually all of the excess voltage above open circuit should be absorbed by the positive. This results in substantially higher currents for VRLA cells on CV charge relative to flooded analogs; the amount of current necessary to overcome the recombination process will be contingent upon cell construction and the resultant recombination efficiency. At some overcharge current, the capacity of the cell for oxygen recombination should be saturated, and the negative should then polarize normally with further voltage increases being distributed between the two electrodes according to their inherent polarizabilities; it has been shown that the polarization behaviour of lead/acid systems can be very sensitive to materials and cell-processing/construction [5]. What might be called 'typical' behaviour for flooded and recombinant cells for a 110 mV 'float' electrode polarization is shown conceptually in Fig. 2. The current increase for the recombinant cell is exaggerated for presentation purposes, and is reported to be of the order of a factor of 2 - 3 over those for flooded analogues [4].

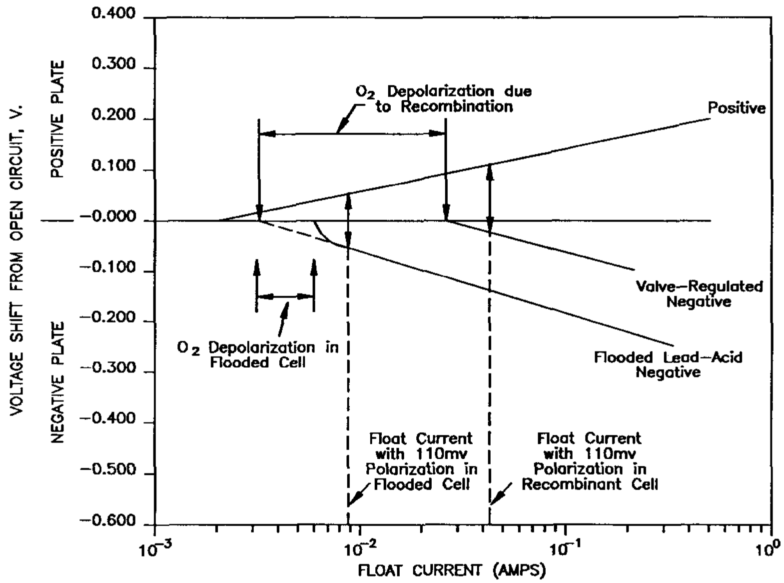

Fig. 2. Polarization behaviour of flooded and recombinant lead/acid cell electrodes as function of overcharge current.

Similar results would be expected for constant-current (CC) charging in that, for a given applied current level, the plate voltages should correspond to values obtained from CV charging. However, at low currents/voltages (typical float conditions) the electrodes are not strongly driven into overcharge and recombination and they may drift and 'hunt' for stable potentials; thus, variable behaviour cell-to-cell is not uncommon, and this is probably the cause for cell-to-cell on-charge variations of 100 - 150 mV in recombinant cell/battery arrays. Some of this variability decreases when cells within a battery have a common gas space for pressure equalization [6], but it is still a substantial problem in VRLA systems.

Figure 3 shows typical CV and CC polarization curves for the same 2 V/2.5 A h 'D' cell, and it can be seen that the curves are roughly similar and do follow some expectations. At low voltages/currents, the positive does absorb the bulk of the voltage increase and the negative plate potential remains fairly constant, though not at, or near, the open-circuit value. Above 2.50 V, or a current of about 200 mA, the positive polarization becomes excessive and the negative begins to 'drag down' towards open circuit. It is believed that this is a thermal effect and is probably the precursor to 'thermal runaway'.

Figure 4 is another view of this process for a 2 V/5.0 A h 'X' cell undergoing successive CC 'steps' from $C/100$ to $C/5$. It can be seen that at low current levels the positive absorbs all of the voltage excursion, while at higher levels the negative is driven into overcharge when the current is

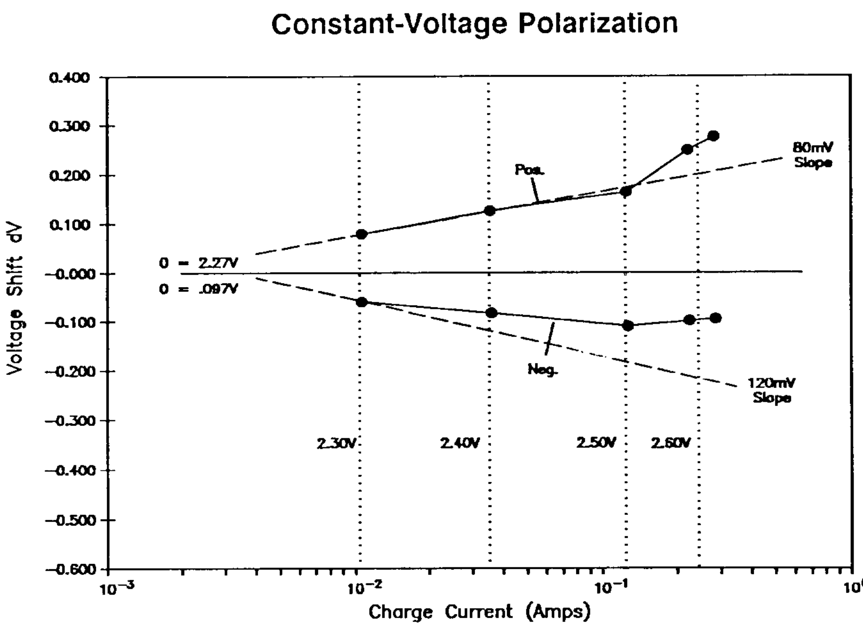

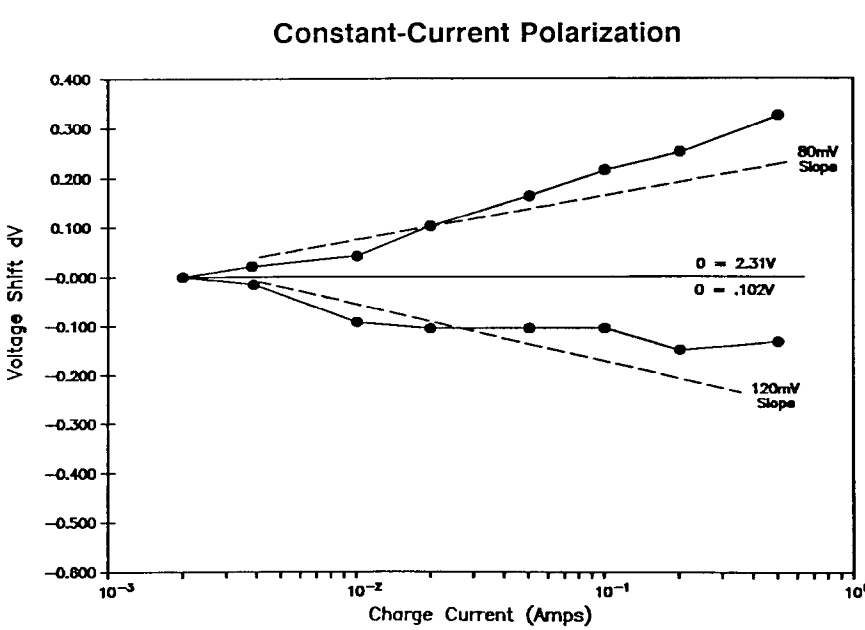

Fig. 3. 'D' single-cell (2 V/2.5 A h) Tafel plots as a function of method of polarization.

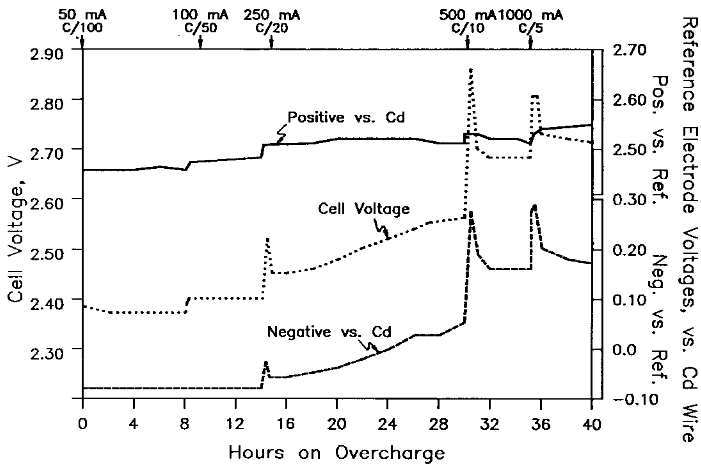

Fig. 4. 'X' single-cell (2 V/5.0 A h) reference-electrode and cell voltages as function of constant-current overcharge level.

stepped, but then drops back down as recombination becomes more dominant. Concurrent temperature monitoring shows that when appreciable currents are passed, cell heating occurs to the point that at the end of the *C*/5 charge period the internal cell temperature is at 48 °C. The full effect of this temperature build-up on the recombination process is not known, but it is qualitatively clear from separate studies that under conditions where high internal temperatures build, either by elevated current levels or by containment of heat, or both, the result on the negative plate is rapid and dramatic: the plate potential drops to near open-circuit values, indicating that recombination and resultant plate oxidation are occurring at very efficient rates (see below).

Gassing studies are consistent with these observations on negative-plate polarization as a function of overcharge rate, as shown in Table 3. These are cumulative gas volumes and they do not really demonstrate the characteristic behaviour shown under CC charge conditions. At low charge levels, gassing is low and steady; as can be seen from the data, it is not a function of vent pressure but rather is probably tied to the cell design and electrolyte distribution. At the *C*/20 rate and above, the gassing rate, cell voltage and negative plate potential are initially high and then drop off as the negative is increasingly depolarized by the recombination process. At the *C*/10 and *C*/5 rates the recombination efficiency is clearly a function of vent pressure, with the high-pressure (production) cell having far and away the best gas-recombination performance. It has been demonstrated that recombination efficiency is a complex factor that cannot be related only to stoichiometric H_2 and O_2 (water) loss [7] but, for illustrative purposes, if the 99 cm^3 of gas evolved by the 35 psi vent pressure cell in Table 3 at the *C*/5 overcharge rate is considered in terms of water loss, then the recombina-

TABLE 3

Gas volumes evolved on constant-current overcharge
(Slit valve variation.)

Overcharge current (mA)	Charge time (h)	Input (A h)	Total gas evolved (cm^3)		
			35 psi cell	12 psi cell	4 psi cell
25 (*C*/100)	67	1.68	75[a]	60[a]	49[a]
50 (*C*/50)	27.3	1.36	14	16	20
125 (*C*/20)	117.4	14.7	61	51	58
250 (*C*/10)	26.7	6.68	27	60	287
500 (*C*/5)	6.3	3.15	99	1118	1189

[a]Cells were not fully charged, some 'finishing' current is involved.

TABLE 4

Gas volumes evolved on constant-current overcharge
(Machined valve stems.)

Overcharge current (mA)	Charge time (h)	Input (A h)	Total gas evolved (cm^3)		
			35 psi cell	15 psi cell	8 psi cell
25 (*C*/100)	29.5	0.74	63[a]	60[a]	8[a]
50 (*C*/50)	65.0	3.25	110	113	58
125 (*C*/20)	26.5	3.31	24	420	38
250 (*C*/10)	48.0	12.0	86	~1300	~1200
500 (*C*/5)	4.4	2.2	53	463	603

[a]Cells were not fully charged, some 'finishing' current is involved.

tion efficiency over the 6.3 h charge period is about 98%. Towards the end of charge, it is actually >99%, since the bulk of the gas liberation is in the first part of overcharge and at the tail end it is relatively low.

Table 4 shows similar data for cells with machined valve stems, and the results are qualitatively similar, though it should be noted that there is considerable variation in gassing characteristics for each cell pair in the 'low', 'medium', and 'high' vent pressure groups.

Long-term overcharge studies with simple cell weighing in lieu of gas collection were also carried out, as shown in Table 5. The same general trends with regard to vent pressures and overcharge levels hold up, but it is interesting to note that for the cells with 'low' and 'medium' vent pressures there were actual weight *gains* on overcharge at the *C*/100 overcharge rate. This has been verified in other testing and it appears that low vent pressure

TABLE 5

Weight loss (gain) for D cells on constant-current overcharge
(Slit valve variation.)

Overcharge current (mA)	Charge time (h)	Input (A h)	Cell weight loss (mg)		
			34 - 42 psi[a]	8 - 11 psi[a]	5 - 6 psi[a]
25 (*C*/100)	72	1.8	24	[c]	(14)[b]
50 (*C*/50)	24	1.2	9	7	2
125 (*C*/20)	24	3.0	13	126	48
250 (*C*/10)	96	24	36	730	564
500 (*C*/5)	48	24	138	1901	1246
Cumulative weight loss (g)			0.161	2.765	1.845

[a]Average values for 3 cells.
[b]Denotes weight gain due to O_2 ingress.
[c]Two cells gained weight (8, 9 psi vent pressures), one lost (11 psi vent pressure).

valves may stay open and allow O_2 ingress either on charge, or even on stand, for vent pressures below about 8 psi.

Separate weight measurements were taken for 'D' cells on open-circuit stand for a 14-day period in the laboratory (23 ± 3 °C). The 'high' vent pressure cells (29 - 41 psi, $n = 10$) had slight weight losses averaging about 4 mg; the 'intermediate' vent pressure cells (slit valves, 8 - 13 psi, $n = 10$) had weight gains averaging 100 mg; the 'low' vent pressure cells (slit valves, 4 - 7 psi, $n = 10$) averaged about 150 mg weight gain. This last weight gain, if it is all in the form of oxygen, corresponds to an uptake of about 105 cm^3 of O_2 — a substantial amount, particularly for a small cell such as this. In larger batteries, oxygen ingress may not be as problematic as in small cells, but any design incorporating low vent pressures ($< \sim 8$ psi) may be susceptible to this problem.

The gassing experiments showed that at low charge levels these cells stayed in the recombination mode, and at higher currents the negative would be driven into overcharge and, in some cases, would be depolarized by oxygen recombination, resulting in reduced gassing levels and negative electrode potentials close to the open-circuit values. In order to get a closer look at the onset of recombination, potentiostatic and constant-current overcharge experiments were carried out.

Figure 5 shows the negative electrode polarization behaviour for three different vent pressures when the positive electrode is potentiostatically stepped from its open-circuit value to a level 100 mV above this. The result is a sharp polarization of the negative and a large burst of current that peaks at ~ 1.6 A; the current and negative plate voltage then rapidly decay, the latter due to a combination of reduced current and some contribution from oxygen recombination. It is interesting to note that the shapes of the decay

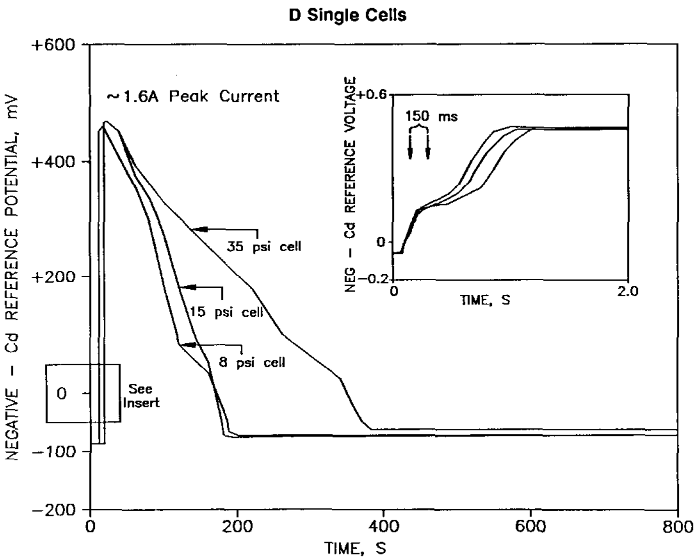

Fig. 5. 'D' single-cell negative-plate polarization curves with 100 mV positive plate potentiostatic step for three different vent pressures.

curves are different for the three cells tested: since the current decay curves were similar in all three cases, the inference is that the cells with the two lower vent pressures are recombining more efficiently. The causes of the inflections and plateaux on these curves are not known at this time.

The overall shapes of the curves are not unexpected, but of particular note is a small area at the beginning of the negative plate polarization which is expanded in the Figure insert. Roughly 150 ms into the experiment there is a plateau at about 100 mV *versus* Cd which then rapidly goes to the hydrogen evolution level at about 450 mV *versus* Cd. This 'jog' in the curve may be the onset of oxygen recombination that momentarily depolarizes the negative but then is rapidly overpowered by the drive to the H_2-evolution level. Taking into account the dimensions and O_2 diffusivities cited in Fig. 1, it is not unreasonable that O_2 recombination would occur on this time scale, with an infinite concentration gradient for oxygen between the positive and negative electrodes once current begins to flow.

In order to get a clearer picture of this process, several constant-current levels were imposed upon 'D' cells with different vent pressures, and again the negative-plate polarization curves were recorded. In terms of diffusion kinetics this is a different process; instead of an initial large supply of oxygen followed by a sharp drop off, the production in these experiments is relatively constant and at variable levels.

Figure 6 shows the family of curves for a cell with a vent pressure of 8 psi; Fig. 7 is for one at 41 psi. Each shows variable behaviour over the current range employed (25 - 2000 mA) and they are clearly different from

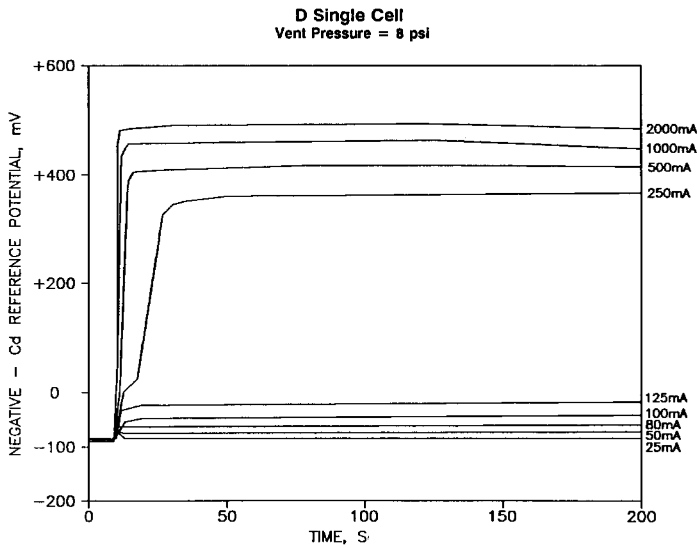

Fig. 6. Negative-plate polarization as function of constant-current overcharge level for 'low' vent pressure cell.

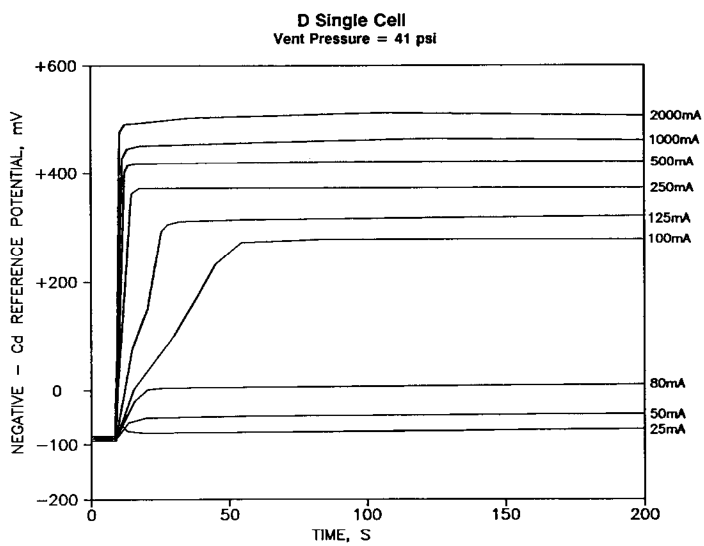

Fig. 7. Negative-plate polarization as function of constant-current overcharge level for 'high' vent pressure cell.

each other. The 8 psi cell shows strong recombination up to the 125 mA ($C/20$) level in that throughout the 200 s charge period the negative plate voltage is constant and close to the open-circuit value of about −0.090 V *versus* Cd. Although it is not obvious from the Figures, there appears to be a competition between the hydrogen-evolution overcharge process and the recombination reaction to control the electrode potential. Thus, the 'jog' attributed to the onset of recombination, and the 'flat' curves at lower current levels, occur at higher potential as the current is increased. In Figs. 6 and 7 there are clearly 'break' points where the plate potential shifts from being dominated by recombination depolarization to being driven into the hydrogen-evolution overcharge reaction as the primary process. At the intermediate levels, there may be a 'mixed potential' situation on the negative plate, with some areas having high levels of recombination and others being in overcharge. At a microscopic level, this may be due to some of the smaller plate pores being filled with electrolyte and the large pores having the desired relatively-thin-film-condition existing.

It is interesting to note that the 'break' points for the 8 psi and 41 psi cells occur at different current levels — roughly $C/10$ and $C/30$, respectively. This appears to be inconsistent with the gassing studies, but it has been found that at virtually all current levels, the high vent pressure cells may be driven into overcharge relatively easily, but they also drop back down into recombination much more readily than the lower vent pressure cells, as shown in Fig. 8 for some longer-term studies at the $C/10$ and $C/5$ rates. These cell voltage excursions are consistent with the gassing data shown in Tables 3 and 4 (these curves correspond to cell data shown in Table 4) and they emphasize the difference in 'high' and 'low' vent pressure cells with regard to recombination behaviour at high charge rates.

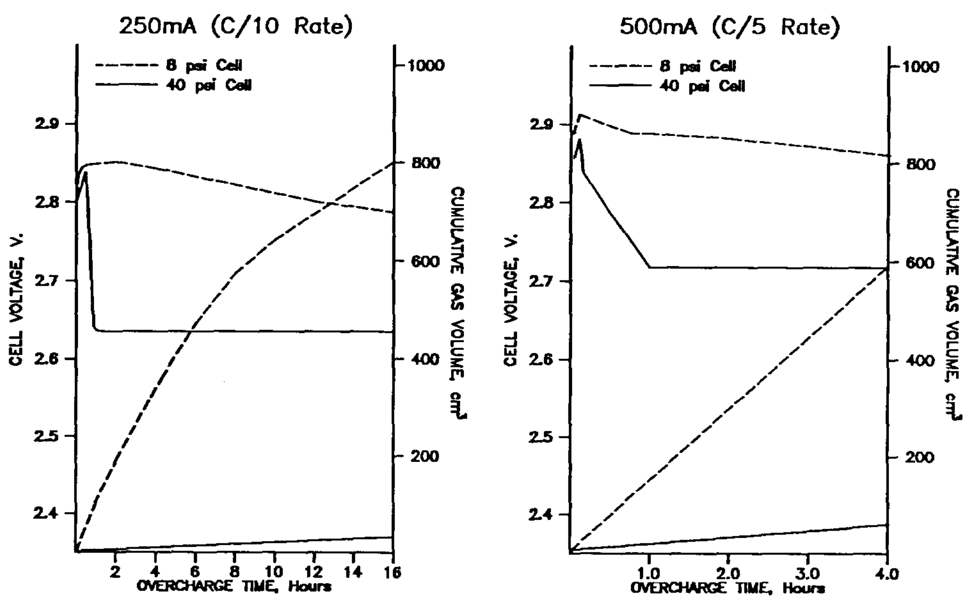

Fig. 8. 'D' single-cell voltages on constant-current charge with concurrent gas collection. Upper traces are cell voltages, lower traces are cumulative gas volumes.

It should be noted that at longer times than shown in Fig. 8 the 'low' vent pressure cells continue to decline in voltage and gassing rate so that, for example, at the $C/10$ rate at 48 h, the cell voltages are only separated by about 40 mV for the two cells, and the gassing rate for the 'low' vent pressure cell has dropped substantially, but is still at appreciable levels. Once again, these data demonstrate that, at high charge rates, higher vent pressures are clearly beneficial in promoting higher recombination efficiencies in these wound cells.

The shapes of the negative plate polarization curves shown in Figs. 5 - 7 are not understood at all well at this time. It is believed that the voltage plateaux around +100 mV *versus* Cd are due to O_2 recombination, but this is not a certainty at this point. Why 'high' vent pressure cells do not appear to recombine as well as 'low' pressure cells at low charge rates, but clearly recombine more effectively at higher charge rates, is also not fully understood. Likewise, the effects of temperature are not wholly delineated, and if, and how, the oxygen cycle can lead to 'thermal runaway' remains to be elucidated.

Studies are now under way looking at flooded, recombinant wound cells with, and without, heat dissipation to shed more light on these processes.

Conclusions

Though this study is clearly only a first, tentative step towards understanding the recombination process in lead/acid cells, and raises more questions than it answers, the following conclusions can be drawn from the data contained herein:

(i) the overcharge process can be effectively studied using reference-electrode measurements in conjunction with other physico-chemical techniques;

(ii) due to the influence of the oxygen recombination process, negative and positive plate polarization curves are considerably more complex than those for flooded systems which adhere to the classical Tafel relationships;

(iii) gassing and polarization behaviour are highly variable, cell-to-cell, for a given cell configuration;

(iv) at low overcharge rates ($\leqslant C/20$), recombination efficiencies are very high and negative plate polarization is minimal; voltage excursions are absorbed largely by the positive; gassing and recombination levels are independent of cell vent pressures, and appear to be governed by cell design and materials' structure and distribution;

(v) at high overcharge rates ($\geqslant C/10$), recombination efficiencies are substantial in all cases, but are clearly higher for high ($> \sim 15$ psi) vent-pressure wound cells, even though negative-plate polarization levels are elevated; with time, these levels decrease and gassing rates correspondingly diminish;

(vi) the 'drag down' of negative-plate voltages at high overcharge levels is believed to be due to thermal effects;

(vii) in some vent-valve designs, low-vent-pressure configurations may allow ingress of atmospheric oxygen;

(viii) a microscopic understanding of the recombination process is largely incomplete at present.

References

1 J. Tafel, *Z. Phys. Chem.*, *50* (1905) 641.
2 P. Rüetschi and J. B. Ockerman, *Electrochem. Technol.*, *4* (1966) 383.
3 W. B. Brecht, *Proc. INTELEC '88, 9th Int. Telecommunications Conf., San Diego, 1988,* IEEE, Piscataway, NJ, p. 35.
4 D. Berndt, *Proc. INTELEC '88, 9th Int. Telecommunications Conf., San Diego, 1988,* IEEE, Piscataway, NJ, p. 89.
5 M. E. Fiorino, F. J. Vaccaro and R. E. Landwehrle, *Proc. INTELEC '88, 9th Int. Telecommunications Conf., San Diego, 1988,* IEEE, Piscataway, NJ, p. 114.
6 D. H. McClelland, T. Uba and L. K. W. Ching, *U.S. Pat. 4,383,011* (1983).
7 J. S. Symanski, B. K. Mahato and K. R. Bullock, *J. Electrochem. Soc.*, *135* (1988) 548.